Astronomical and Astrophysical Transactions (*AApTr*), 2024, Vol. 34, Issue 4, pp. 427–438,
ISSN 1055-6796, Photocopying permitted by license only, ©Cambridge Scientific Publishers

Construction of asteroid search ephemerides based on the uncertainty clouds

T.Yu. Galushina[1,*], O.N. Letner[1], A.V. Shein[2], E.S. Bakanas[3], P.A. Levkina[3]

[1] *Tomsk State University, 36 Lenin Ave., Tomsk, 634050, Russian Federation*
[2] *Terskol Branch of the Institute of Astronomy, Russian Academy of Sciences, 81 Elbrus Ave., Ap. 33, Tyrnyauz, Kabardino-Balkaria Republic, 361603, Russian Federation*
[3] *Institute of Astronomy of the Russian Academy of Sciences, 48 Pyatnitskaya Str., Moscow, 119017, Russian Federation*

Received 29 November, 2024; accepted 4 December, 2024

The paper is devoted to the problem of constructing search ephemerides for asteroids with poorly determined orbits. It describes the method of their construction based on the uncertainty cloud of the asteroid's position. We also present the results of the successful application of the method to obtain astrometric observations of five asteroids on the Zeiss-2000 telescope of the Terskol Observatory Core Shared Research Facility in 2021–2023. Particular attention is paid to the object 2022 SG9 observed during two sessions, which made it possible to halve the size of the uncertainty cloud in coordinates and velocities and led to a decrease in the volume of the confidence ellipsoid by two orders of magnitude. In addition, a study of the orbital evolution of this small body was carried out, which demonstrated regular transitions between classes of near-Earth and Mars-crossers asteroids, as well as the potential possibility of approaching Jupiter.

Keywords: Near-Earth asteroids, astrometric observations, uncertainty cloud, orbital evolution

1 Introduction

Currently, several thousand asteroids are discovered every year, a significant portion of which belong to the class of near-Earth asteroids (NEA). However, to reliably predict the motion, it is necessary to observe the object in several oppositions, which, unfortunately, is not always possible. An insufficient number of observations lead to a large uncertainty in the position of the asteroid both in space and on the celestial sphere, which significantly complicates its subsequent observations. One possible solution to this problem is to estimate the size and position of the uncertainty cloud on the celestial sphere and scan the area it occupies during observations.

*Email: tatyana.galushina@mail.tsu.ru

We have previously developed an algorithm and programs for constructing overview (search) ephemerides based on the uncertainty cloud of the asteroid's position (Bykova et al., 2007a; Bykova et al., 2007b; Bykova et al., 2012). In this paper, we present some modifications of a previously developed programs allowing automatic estimation of the size of the uncertainty cloud on the celestial sphere for a large number of asteroids, as well as the results of testing the proposed method during the observation session with the Zeiss-2000 telescope at Terskol Observatory Core Shared Research Facility. In addition, the dynamics of the asteroid 2022 SG9, calculated based on the observations obtained, is considered.

2 Algorithm and program for constructing search ephemerides

The algorithm for calculating the search ephemeris of an asteroid based on the uncertainty of its position includes the following blocks:

1. constructing the initial uncertainty cloud of the asteroid's position based on the results of observations obtained before the current session;
2. constructing the uncertainty cloud of the asteroid at the time of the upcoming observation t_2;
3. projecting the uncertainty cloud onto the celestial sphere at the time of the upcoming observation t_2.

In most cases, linear methods are sufficient to construct the initial uncertainty cloud (Syusina et al., 2012). Then, using the covariance matrix, obtained as a result of orbit fitting, clones distributed according to the normal law are generated. The number of particles depends on the size of the uncertainty region, the time interval from the epoch of the best conditionality t_0 to the observation time t_2, and the required accuracy. Usually, 100 to 1000 clones are sufficient. By numerically integrating the equations of motion of each clone, the uncertainty cloud in space is displayed at the time of observation, and then, its projection onto the celestial sphere is constructed using mathematical transformations. The force model depends on special features of an asteroid orbit.

The initial implementation of the described algorithm can be found in Bykova et al. (2007a,b). They provide a description of the programs for calculating the overview (search) ephemerides. In the past few years, the programs have undergone significant changes and updates and have been combined into the IDA software described in detail in Galushina and Letner (2021).

Previously, when it was necessary to calculate search ephemerides, multiple manual launches of subsystems were required, which led to significant time costs. In this work, the task was set to automate this process. We present the results of using the method to obtain astrometric observations of five asteroids on the Zeiss-2000 telescope of the Terskol Observatory Shared Use Center in 2021–2023.

The automation consists in creating a control program that sequentially changes the input files and calls the necessary subsystems. Figure 1 schematically shows the stages of the work. Here, t_0 is the arithmetic mean of the observation times, t_1 is the epoch of the Bowell catalog (Bowell et al., 1994), and t_2 is the observation moment. Observations of asteroids from the Minor Planet Center website

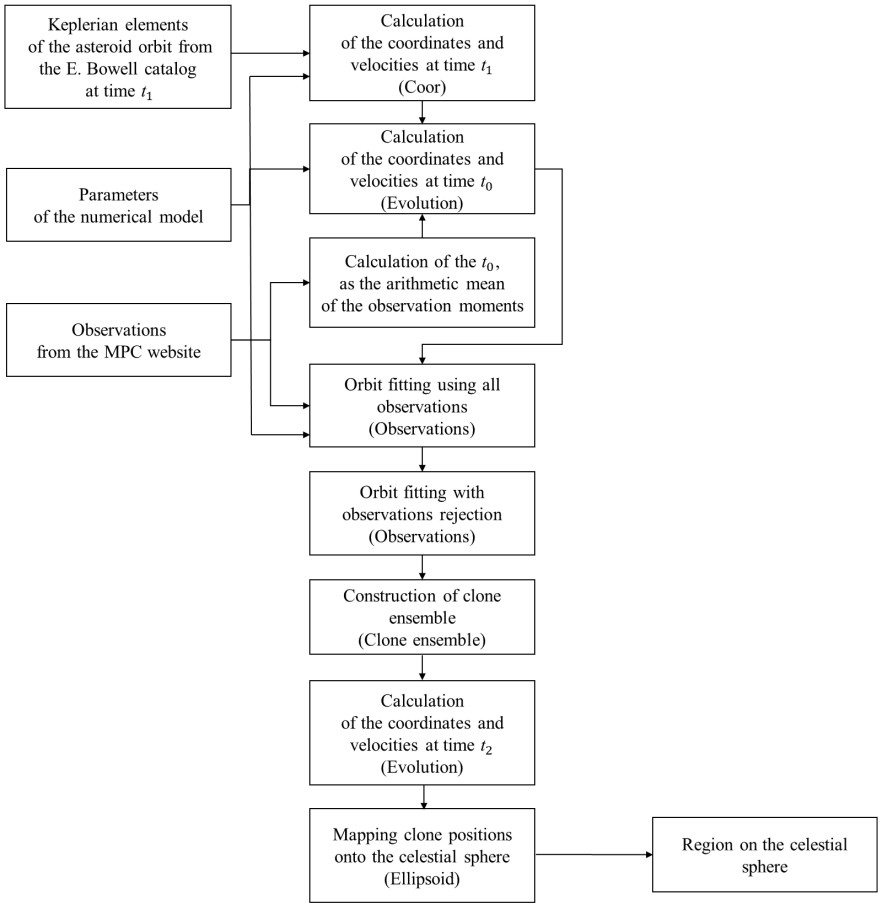


Figure 1 Stages of the process of constructing search ephemerides.

(https://minorplanetcenter.net/) and Keplerian elements from the E. Bowell catalog (Bowell et al., 1994) at time t_1 are used as input data. After starting the program, the process is automatically repeated for a given number of asteroids. The name of the subsystem used is written in brackets on the diagram.

3 Approbation of the methodology for construction search ephemerides on real observations

The approbation was carried out over four sessions from October 2021 to January 2023. First, a selection of near-Earth asteroids was made from the E. Bowell catalog according to the following conditions: the apparent magnitude $m \leq 21^m$ and the altitude above the horizon $h \geq 35°$. The choice of these conditions is due not only to the capabilities of the telescope, but also to the fact that the need to use long exposures

Table 1 General data on observation sessions.

Data	N	A_{con}	A_{obs}
28.10–6.11.2021	4	336	1
28.06–9.07.2022	4	323	2
18.10–6.11.2022	7	227	1
14–27.01.2023	7	589	2

and to make a photo low above the horizon significantly complicates scanning areas of the sky. In addition, large errors in determining the orbit can lead to significant errors in determining the apparent magnitude and altitude, which will cast doubt on the possibility of observing such objects.

Table 1 shows the dates of the observation sessions, the number of nights in each session N, the number of asteroids satisfying the above conditions A_{con}, and the number of asteroids for which observations were obtained A_{obs}. The asteroids under consideration can be divided into three classes:

1. objects, whose uncertainty region of position in the sky is smaller than the field of view of the Zeiss-2000 telescope ($11' \times 11'$);
2. objects, whose uncertainty region is several times larger than the field of view;
3. objects, whose uncertainty region is tens and hundreds of times larger than the field of view.

The first class is the most numerous, it does not require the use of search ephemerides. For the third class of objects, the use of search ephemerides is impractical. In fact, they are lost and can only be accidentally rediscovered. The subject of this study are asteroids of the second class.

To calculate the ephemerides of the selected asteroids, the EPOS software package (L'vov, Tsekmeister, 2012) was used. According to the sizes of the uncertainty regions, the search for objects was carried out in the ephemeris field and, with overlap, in neighboring fields. In each observation session, we were forced to limit ourselves to 1-2 objects from the second class, because scanning the neighboring fields takes a significant amount of time, and other tasks were also solved on the selected nights.

Calibration and processing of the images were carried out using the Apex II software package (Devyatkin et al., 2010). Processing of the obtained CCD images includes calibration of the images using calibration frames, as well as successful identification of the image using the UCAC5 star catalog. The Apex II software package was also used for the primary calibration of the images.

Table 2 shows the sizes of the uncertainty clouds for the asteroids selected for observations. Here, $\Delta\alpha$ and $\Delta\delta$ are the uncertainties in right ascension and declination, respectively (in arcmin), m is the apparent magnitude. It should be noted that the uncertainty clouds of asteroids 2003 MW7 and 2014 NV63 have significant sizes. However, just a couple of days before our summer observing session of 2022, observations of these objects appeared in the Minor Planet Center (MPC, https://minorplanetcenter.net/) database, which made it possible to detect them in the sky. During the autumn session, a similar situation occurred with the asteroids of the second class. As a result of new observations, the uncertainty became less

Table 2 Sizes of uncertainty clouds for some NEAs.

Asteroid	Data	m	$\Delta\alpha$, $'$	$\Delta\delta$, $'$
2014 WB363	03.11.2021	20.5	16	54
2003 MW7	27.06.2022	19.2	772	4134
2014 NV63	27.06.2022	19.9	509	3677
2022 SG9	17.10.2022	20.4	0.3	5
2014 BQ8	15.01.2023	6.8	6.9	9.5
2022 SG9	15.01.2023	19.0	83.1	76.5
			0.02	0.3

than $1'$. Therefore, the asteroid 2022 SG9 was chosen for observations, the size of the uncertainty region in declination for the positions of which was about half the field of view of the telescope. The last row shows the uncertainties of the position on the celestial sphere of 2022 SG9 without and with taking into account the observations at the Terskol Observatory in October 2022. It is clear that the use of our observations made it possible to reduce the uncertainty by several orders of magnitude.

The results of the observations are presented in Table 3, where m is the apparent magnitude, N_f is the number of images, in which the observed object was detected during processing by the Apex II software package, N_σ is the number of images with acceptable (O–C), $(\text{O–C})_\alpha \cos\delta$ and $(\text{O–C})_\delta$ are the average residuals of N_σ observations in right ascension and declination, respectively.

Table 3 Observation results.

Object	Observation data	m	N_f	N_σ	$(\text{O–C})_\alpha \cos\delta$, $''$	$(\text{O–C})_\delta$, $''$
2014 WB363	04.11.2021	20.8	17	9	0.10	0.05
	28.06.2022	20.7	5	5	0.47	0.28
2003 MW7	29.06.2022	20.6	8	8	0.42	0.41
	09.07.2022	20.4	3	3	0.14	0.27
2014 NV63	09.07.2022	20.2	6	5	0.10	0.27
	25.10.2022	20.3	33	33	0.06	0.05
	29.10.2022	20.2	9	9	0.08	0.11
2022 SG9	01.11.2022	20.2	24	24	0.09	0.08
	30.01.2023	18.7	10	10	0.32	0.11
	31.01.2023	18.6	29	28	0.03	0.05
2014 BQ8	14.01.2023	20.7	8	4	0.33	0.38
	16.01.2023	20.6	10	6	0.30	0.34

The accuracy of the obtained observations was assessed using the method described in Galushina and Skripnichenko (2013), which consists of the following: the obtained observations were added to the general set and the orbit fitting process was carried out with rejection according to the three sigma rule. Table 3 presents the average residuals of the observations remaining after rejection. It should be noted

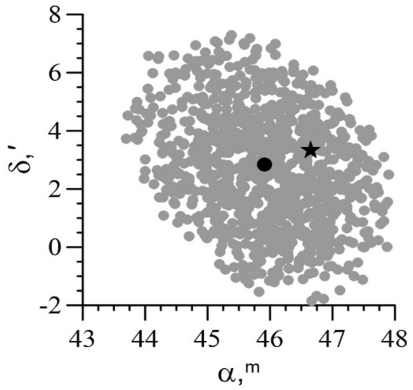


Figure 2 Uncertainty cloud of asteroid 2022 SG9 on the celestial sphere at the time of observations on October 25, 2022.

that they are highly accurate, despite the fact that most asteroids were weaker than 20^m at the time of observations.

Asteroid 2022 SG9 deserves special attention – it was discovered on September 19, 2022, and was observed for only 4 nights before our observations in October 2022. As an example of constructing the search ephemerides, Figure 2 shows the uncertainty cloud of this object on the celestial sphere at the time of the first observation at the Terskol Observatory. The cloud is presented in the form of 1000 clones, the black dot shows the position of the nominal particle, and the asterisk shows the actually observed position of the asteroid. Equatorial coordinates α and δ are given in arcmin, the zero value corresponds to $\alpha = 23^h$ and $\delta = 82°$. The cloud occupies almost the entire field of view of the telescope. The observed position of the asteroid does not coincide with the nominal one, but is located inside the cloud.

Table 4 Results of orbit improvement for asteroid 2022 SG9 based on observations of the year 2022.

N	ΔT, days	σ, $''$	$\sigma(x_0)$, au	$\sigma(v_0)$, au/day	V_e, au^6/day^3
19	3.34	0.17	$5.02{\cdot}10^{-3}$	$6.00{\cdot}10^{-5}$	$1.14{\cdot}10^{-33}$
45	43.00	0.33	$5.60{\cdot}10^{-5}$	$6.30{\cdot}10^{-7}$	$2.16{\cdot}10^{-40}$

Thanks to the Terskol observations in October 2022, it was possible to increase the arc length by more than a month and significantly reduce the uncertainty region. The results of the orbit improvement based on different sets of observations are presented in Table 4, where N and ΔT are the number and interval of observations, σ is the mean-square error, $\sigma(x_0)$ and $\sigma(v_0)$ are the mean-square errors of coordinates and velocity components, respectively, and V_e is the volume of the confidence ellipsoid in the six-dimensional space of coordinates and velocity components. The first row corresponds to the results obtained from the observations of 2022 year presented on the MPC website, the second one corresponds to the results with the addition of measurements obtained at the Terskol Observatory. It is clear from Table 4 that using the observations we obtained increased the arc length by 13 times, reduced the

uncertainty in the coordinates and velocity components by 2 orders of magnitude, and reduced the size of the confidence ellipsoid by 7 orders of magnitude.

Prior to our next session in January 2023, the 2022 SG9 had been observed by ATLAS–HKO, which meant that for this asteroid no search ephemeris were required in the second session. However, according to the MPC website data, its orbital uncertainty was 4, meaning that continued tracking was required.

4 Study of the orbital evolution of asteroid 2022 SG9

According to MPC data for July 2024, asteroid 2022 SG9 has 45 observations over a time interval of 209 days (09/19/2022 – 04/17/2023). The results of its orbit calculation for February 25, 2023, presented on the MPC website, show that, having a perihelion distance of 1.309 au, it belongs to the class of Mars-crosser asteroids (MCA). At the time of our observations at the Terskol Observatory, the asteroid belonged to the class of near-Earth asteroids, but after its orbit was improved in 2023, the class changed to MCA. In order to identify the features of its motion, including the transition from one class of objects to another, we constructed and studied its orbital evolution.

At the first stage, a study was conducted of the influence of the observations obtained by us at the Terskol Observatory on the improvement of the asteroid's orbit. Our observations did not extend the observation interval, but increased the number of observations by 104 moments.

Table 5 shows the results of fitting the orbit of asteroid 2022 SG9 based on observations presented on the MPC website (first row) and those with the addition of the Terskol observations (second row). The asteroid orbit was improved at the time of 12/12/2022, equidistant by 5 days from the arithmetic mean of the observation moments for the two sets under consideration. In the process of improving according to the 3σ rule, one observation was excluded from the group of observations only from MPC, and two moments were excluded from the group of observations with the addition of Terskol observations. It is evident from Table 5 that the use of our observations made it possible to halve the size of the uncertainty cloud for coordinates and velocities and led to a decrease in the volume of the confidence ellipsoid by two orders of magnitude.

Table 5 Results of orbit improvement for asteroid 2022 SG9 based on MPC observations and with the addition of Terskol observations.

N	ΔT, days	σ, $''$	$\sigma(x_0)$, au	$\sigma(v_0)$, au/day	V_e, au^6/day^3
44	209	0.2680	$2.058{\cdot}10^{-6}$	$2.380{\cdot}10^{-9}$	$1.036{\cdot}10^{-44}$
147	209	0.3229	$1.021{\cdot}10^{-6}$	$1.145{\cdot}10^{-9}$	$8.686{\cdot}10^{-46}$

Based on the improvement results for two cases from Table 5, a nominal orbit was formed and its evolution was constructed by numerical integration of the equations of motion using the Lobbie method (Avdyushev, 2022) and the IDA software package (Galushina, Letner, 2021). The study interval was determined by the integration accuracy not exceeding 10^{-9} au. During the integration process, perturbations from

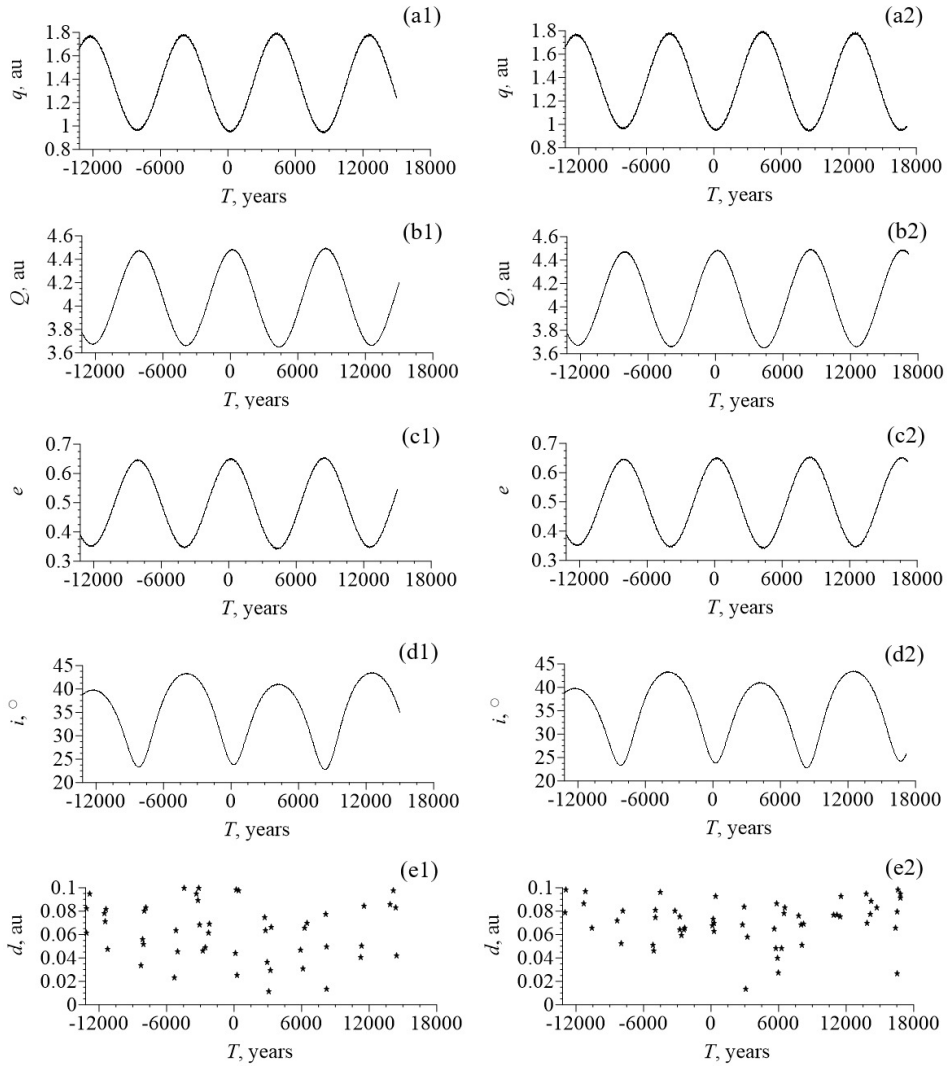


Figure 3 Orbital evolution of asteroid 2022 SG9.

all major planets of the Solar System, the Moon, three large asteroids (Ceres, Pallas, and Vesta), relativistic effects of the Sun, and the oblateness of the Sun were taken into account. The coordinates of the major planets were taken from the Jet Propulsion Laboratory (JPL) Planetary Development Ephemeris DE441 (Park et al., 2021).

Figure 3 shows the results of studying the evolution of the orbital elements of nominal particles formed by processing two groups of observations: 1) observations taken from the MPC site (graphs on the left) and 2) observations from the MPC site with the addition of our observations at the Terskol Observatory (graphs on the right). When integrating into the past, the study interval for both cases was limited by the size of the Planetary Ephemeris DE441. It is important to note that the integration

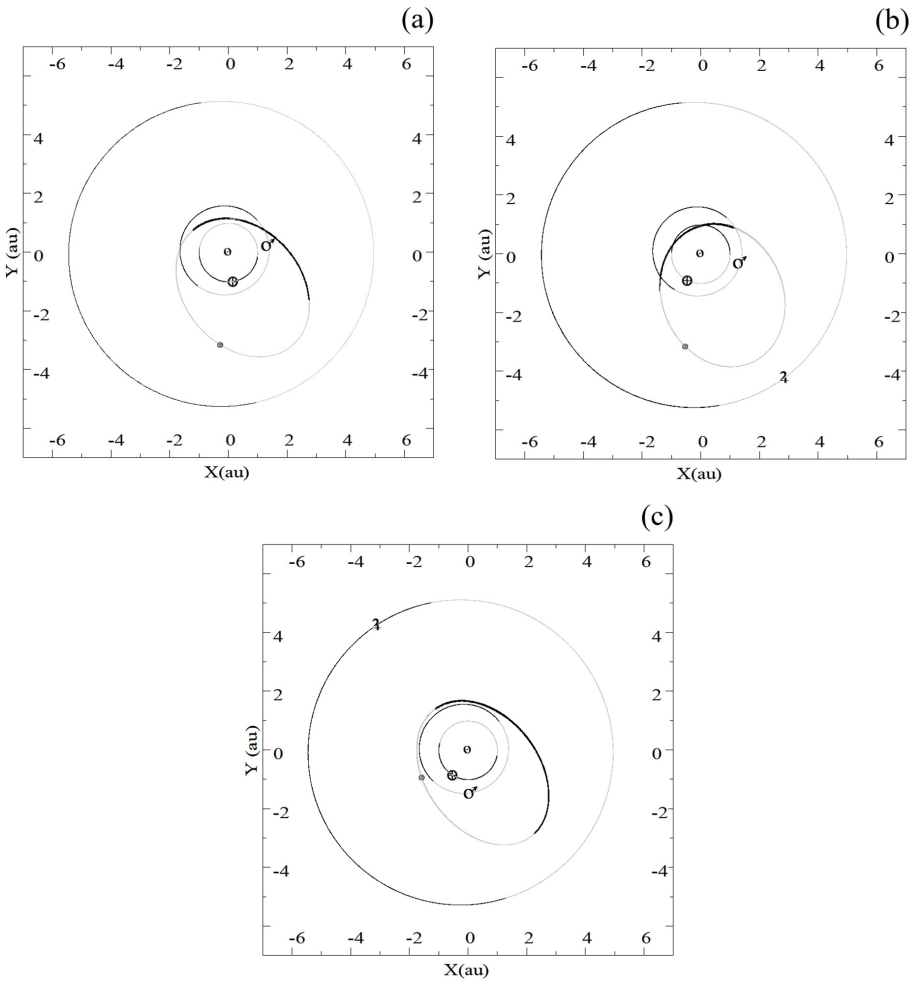


Figure 4 Projection of the orbit of asteroid 2022 SG9 and planets on the ecliptic plane at different moments in time.

accuracy for the nominal orbit taking into account only the MPC observations at that moment had the maximum permissible value, while for the orbit with the addition of the Terskol observations, the margin of error was two orders of magnitude. When integrating into the future for case 1), the study interval was about 13,000 years, while the addition of the Terskol observations made it possible to expand the study interval to the end of the Planetary Ephemeris (about 15,200 years) with a margin of error of one order of magnitude.

It is evident from Figure 3 that the change in the composition of observations did not affect the nature of the evolution of the orbital elements, but allowed us to consider the motion of the asteroid over an extended time interval. The evolution of the perihelion distance (Figure 3(a1) and Figure 3(a2)) demonstrates regular secular oscillations of q from 0.96 to 1.78 au and back with a period of approximately

8000 years. This feature of the orbit of asteroid 2022 SG9 allows it to belong to different classes of objects depending on the time of consideration of its features. The evolution of the aphelion distance Q (Figure 3(b1) and Figure 3(b2)) also shows a significant spread of its values (from 3.7 to 4.5 au), which indicates that the asteroid is potentially capable of interacting with the Earth, Mars, and Jupiter. But at the same time, quite a large inclination and mutual arrangement of the nodes of orbits of asteroid and planets lead to the fact that throughout the entire study interval the object avoids approaches to all the major planets except Mars. Approaches to Mars in both cases (Figure 3(e1) and Figure 3(e2)) occur regularly, both when integrating into the past and when integrating into the future, although their number and distance to the planet differ slightly. The closest approach of about 0.01 au to the planet will occur in 3080.

Figure 4 shows the projections of the orbits of an asteroid and some planets (Earth, Mars, and Jupiter) onto the ecliptic plane at different points in time. In graphs (a), (b), and (c), the orbit is shown for July 2024, for April 4, and for June 4102, respectively. The black lines show the orbits above the ecliptic plane, and the gray lines show the orbits below the ecliptic plane.

When choosing the time moments for displaying the projections of the asteroid's orbit, we were guided by the values of the perihelion and aphelion distances. It is clear from the figure that, having the minimum value of q Figure 4(b), the nodes of the orbit are located near the orbit of Mars and far from the orbit of the Earth. Figure 4(c) corresponds to the maximum value of the perihelion distance, and Figure 4(a) shows the current location of the orbits. The position of the nodes of the orbit does not allow the asteroid to approach either the Earth or Jupiter, although this is potentially possible. All the projections shown demonstrate the interaction of the asteroid with Mars.

5 Conclusions

This paper describes an algorithm and a program for calculating search ephemerides of asteroids based on the uncertainty of their position, which make it possible to automatically estimate the size of the uncertainty cloud on the celestial sphere for a large number of asteroids. The results of testing the proposed method are presented using the example of observations on the Zeiss-2000 telescope of the Terskol Observatory Core Shared Research Facility. The testing was carried out during four sessions in the interval from October 2021 to January 2023. Five asteroids were selected for observations, the region of uncertainty of their position in the sky of which is several times larger than the field of view of the Zeiss-2000 telescope (2014 WB363, 2003 MW7, 2014 NV63, 2014 BQ8, 2022 SG9). The assessment of accuracy of the obtained observations by improving the orbits of asteroids with rejection according to the three sigma rule showed that the observations remaining after rejection have high accuracy and lead to a significant reduction in the uncertainty cloud.

The dynamics of asteroid 2022 SG9, calculated based on observations from the MPC website and our observations, is considered in detail. Our observations did not lead to an expansion of the interval, but increased the number of observations

by 104 moments, which allowed us to halve the size of the uncertainty cloud in coordinates and velocities and led to a decrease in the volume of the confidence ellipsoid by two orders of magnitude.

Based on two groups of observations: only from the MPC site and with the addition of our observations, the initial parameters of the nominal orbit were formed and their orbital evolution was studied. The change in the composition of observations did not have a significant effect on the evolution of the orbital elements, but allowed us to consider the motion of 2022 SG9 over an extended time interval. The asteroid's orbit experiences regular fluctuations in perihelion and aphelion distances over time, but in the time interval under consideration, asteroid approaches only to Mars.

ACKNOWLEDGEMENTS

The research was carried out within the state assignment of Ministry of Science and Higher Education of the Russian Federation (theme No. FSWM-2024-0005). The results of observations are obtained on Large-Scale Research Facility "Telescope Zeiss-2000" of Terskol Observatory Core Shared Research Facility, Institute of Astronomy RAS. This research used data or services, or both provided by the Minor Planet Center of the International Astronomical Union. This research used NASA's Astrophysics Data System and Scopus (Elsevier).

References

Avdyushev V. A. (2022) Sol. Sys. Res., 56, 32
Bowell E., Muinonen K., Wasserman L. H. (1994) ACM 479, 2789
Brown W. R., Geller M. J., Kenyon S. J., Kurtz M. J. (2005) ApJ, 477
Bykova L. E., Galushina T. Yu., Baturin A. P. (2007a) Izv. Vuzov. Fizika, 50, 5
Bykova L. E., Galushina T. Yu., Baturin A. P. (2007b) Izv. Vuzov. Fizika, 50, 13
Bykova L. E., Galushina T. Yu., Baturin A. P. (2012) AApTr, 27, 489
Galushina T. Yu., Skripnichenko P. V. (2013) Izv. Vuzov. Fizika, 56, 51
Galushina T. Yu., Letner O. N. (2021) AApTr, 32, 355
Devyatkin A. V., Gorshanov D. L., Kouprianov V. V., Verestchagina I. A. (2010) Sol. Sys. Res., 44, 68
L'vov V. N., Tsekmeister S. D. (2012) Sol. Sys. Res., 46, 177
Park R. S., Folkner W. M., Williams J. G., Boggs D. H. (2021) AJ, 161, id.105
Syusina O. M., Chernitsov A. M., Tamarov V. A. (2012) Sol. Sys. Res., 46, 195